On the Relative Stability of Cobalt- and Nickel-Based Amidinate Complexes Against β-Migration

JIAYE LI,[1] JINPING WU,[1] CHENGGANG ZHOU,[1] BO HAN,[1] XINJIAN LEI,[2] ROY GORDON,[3] HANSONG CHENG[4]

[1]*Institute of Theoretical Chemistry and Computational Materials Science, China University of Geosciences Wuhan, Wuhan, People's Republic of China 43007*

[2]*Air Products and Chemicals, Inc., 1969 Palomar Oaks Way, Carlsbad, CA 92011*

[3]*Department of Chemistry and Chemical Biology, Harvard University, Cambridge, MA 02138*

[4]*Air Products and Chemicals, Inc., 7201 Hamilton Boulevard, Allentown, PA 18195*

Received 4 April 2008; accepted 9 July 2008
Published online 16 October 2008 in Wiley InterScience (www.interscience.wiley.com).
DOI 10.1002/qua.21880

ABSTRACT: We present a first-principles study on the relative stability of cobalt- and nickel-based amidinate complexes against β-migration using density functional theory. Factors that influence the reactivity of these compounds were carefully addressed and the calculated molecular structures are in excellent agreement with the available crystal structural data. Reaction energies as well as activation barriers of β-migration were evaluated. The predicted relative stability of the selected compounds is consistent with experimental observations. © 2008 Wiley Periodicals, Inc. Int J Quantum Chem 109: 756–763, 2009

Key words: β-migration; amidinate complexes; ALD

Correspondence to: H. Cheng; e-mail: chengh@airproducts.com

Contract grant sponsor: National Natural Science Foundation of China for Youth.
Contract grant number: 20703040.
Contract grant sponsor: Air Products and Chemicals, Inc.

Introduction

Copper has been used as a replacement of aluminum as an interconnecting material in the microelectronic devices [1]. To prevent copper from diffusing into the Si/SiO_2 substrate, "diffusion barriers," such as metals, and metal nitrides between Cu layers and substrates have been utilized [2, 3]. Unfortunately, it has been observed in many experiments that copper tends to agglomerate on surfaces of some well-performed diffusion barrier materials such as WN and TaN [4–6]. One of the solutions to this problem is to insert a transition metal thin layer between the copper film and the barrier layer as a "glue" that is not only stable on the barrier surfaces but also binds with the copper film strongly to prevent copper aggregation [6, 7]. The current technology to deposit the metal films primarily utilizes physical vapor deposition techniques [8]. However, with increasingly reduced feature size of semiconductor devices, atomic layer deposition (ALD) method is on its way to become the preferred technology for metal deposition due to its potential capability to develop uniform and conformal metal films [9–13]. Unlike chemical vapor deposition technology [14], an ALD process involves well-controlled cycles that allow precursors to be reacted only onto the surface of a substrate and subsequently form thin films with liberation of the resulting ligands. It has been shown that ALD process in general provides good control of stereochemistry, uniform thickness over a large area and good step coverage for high aspect ratio substrates [9, 15–17].

Precursors used to deposit metal films via an ALD process vary in a wide range with ligands made of halides, β-diketonates, alkylamides, amidinates, alkyls, and cyclopentadienyls [13, 15, 18–23], among which amidinate-based precursors can work at a relatively low temperature and are versatile [24]. The reactivity can be tuned by varying the ligand structures [18, 25, 26]. Recently, Gordon and coworkers developed several amidinate-based novel precursors for deposition of Cu, Co, and Ni films [26, 27]. A few issues on precursor stability at ALD conditions arose, resulting in deactivation of these molecules on deposition on surfaces. It was deemed that the instability might be associated with the β-H migration from the ligand side chains to the transition metal atom, such as Ni and Co. It was also found experimentally that the reactivity of amidinate compounds is affected by both the electronic properties of the ancillary ligand (bonding strength) and the size of the migrating group [26, 27]. We recently performed extensive quantum-chemical calculations using density functional theory (DFT) to quantitatively examine whether β-H migration is indeed responsible for the instability of precursors. The computational results were briefly reported in a recent communication [28]. We showed that the migration process is thermochemically endothermic; however, for $Ni(^{i}Pr\text{-}MeAMD)_2$ the reaction is close to thermal neutral. The relatively moderate activation barrier allows β-H migration for $Ni(^{i}Pr\text{-}MeAMD)_2$ to occur, leading to precursor instability at ALD delivery temperatures. It was found that replacing H atoms with methyl groups can substantially stabilize the precursors against β-H migration.

β-H migration in amidinate precursors gives rise to formation of metal hydride, leading to dissociation of N—M bond (M = Ni, Co). An interesting question arises: can β-H migration be prevented by enhancing the interaction between N and the metal center? Chemically, it is possible that the enhancement can be realized by introducing appropriate substituting groups in the ligands [18, 25, 26]. The purpose of the present study is to investigate the effects of the substituting groups in the amidinate ligands on the relative stability of Ni- and Co-based precursors. Besides β-H migration, we also explored the possibility of methyl group migration. The electronic and steric effects on functional group substitution were systematically examined. Theoretical understanding of these effects is important for design and development of novel ALD precursors for semiconductor applications.

Computational Details

The electronic structure calculations were performed using DFT that employs an exchange-correlation functional proposed by Perdew-Wang (PW91) [29–31]. To deal with the unpaired electrons of the transition metal complexes, a spin-polarization scheme was utilized. A double numerical atomic basis set augmented with polarization functions was used to describe the valance electrons, whereas an effective core potential (ECP) was employed to represent the core electrons. Full electron calculations were also conducted and the results were compared with the data obtained with ECP calculations. The calculated maximum differences of bond distances and bond angles are within

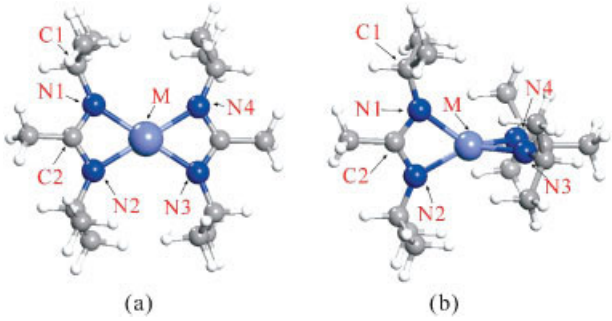

FIGURE 1. The bis-amidinate based first row bivalence transition metal complex. (a) Planar configuration and (b) tetrahedron configuration. [Color figure can be viewed in the online issue, which is available at www.interscience.wiley.com.]

0.004 Å and 0.025°, respectively. The calculated reaction energies of full electron calculations are in general lower than the corresponding ECP values by about 5 kcal/mol, although the trend remains the same, suggesting that the ECP method is essentially adequate. We subsequently performed full energy minimization on all molecular structures without imposing symmetry constraints. On obtaining equilibrium structures of reactants and products, we further calculated transition state (TS) structures utilizing the linear synchronous transit and quadratic synchronous transit search schemes followed by full TS structure optimization with the Newton-Raphson method [32]. The resultant TS geometries were confirmed by the fact that only one imaginary frequency, whose normal mode points to the structures of reactants and products, was obtained. Hirshfeld charge analysis was utilized to understand the charge flow on β-group migration. The computational methods were implemented in DMol^3 package.

Results and Discussions

The bis-amidinate-based complexes of the first row bivalence transition metal ions usually adopt a square planar or a tetrahedron geometry as shown in Figure 1. The tetrahedron structure is often found in Mn(II)-Co(II) compounds [26, 33–35], whereas for Cr(II) and Ni(II) complexes both geometries have been observed [33, 36]. Gordon and coworkers synthesized Co/Ni (^{i}Pr-MeAMD)$_2$ compounds with a distorted tetrahedron geometry [26], whereas a distorted square planar Ni bis-amidinate-based complex was recently prepared by Hessen and coworkers [37]. DFT calculations at the B3LYP/SV level confirmed that the interligand repulsion can be reduced in the planar molecule by adjusting the conformation of substituents on the N atoms [37].

For convenience of description, we use the schematic structures shown in Figure 2 to represent the two structural configurations. Here R and R′ represent substituents in the side chains. Specific groups used in our calculations are also indicated in the figure. To understand the relative stability of the planar and tetrahedron configurations of the amidinate complexes, we first calculated the structures of Co/Ni (^{i}Pr-MeAMD)$_2$, which were synthesized by Gordon and coworkers [26]. Both planar and tetrahedron configurations were obtained [26, 33]. Our calculations yield both geometries for Co/Ni (^{i}Pr-MeAMD)$_2$ in good agreement with the available experimental results as shown in Table I, where the main bond parameters are displayed [28]. The calculated results indicate that the tetrahedron configuration of Co(^{i}Pr-MeAMD)$_2$ and Ni(^{i}Pr-MeAMD)$_2$ are 6.28 kcal/mol and 6.02 kcal/mol more stable than the corresponding planar configuration as shown in Table II. To further understand the relative stability, we replaced the ^{i}Pr groups from the amidinate complexes with H atoms to

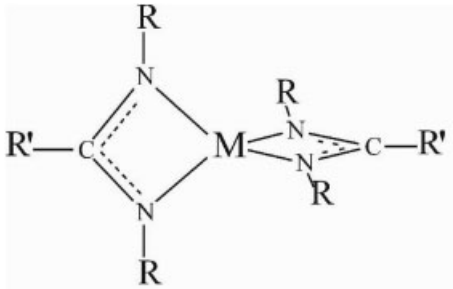

FIGURE 2. Schematic view of Co/Ni(R-R'AME)$_2$. R and R′ represent the substitution groups on N and C of the amidinate ligand. ^{i}Pr represents the iso-propyl group, ^{t}Bu is for the tert-butyl group, TFEt for the trifluoroethyl group, Me for the methyl group, and Et for the ethyl group. M represents Co or Ni.

TABLE I

The optimized bond parameters of planar and tetrahedron Co/Ni(H-HAMD)$_2$ and Co/Ni(^{i}Pr-MeAMD)$_2$ complexes.

	Bis(H-HAMD)		Bis(^{i}Pr-MeAMD)	
	Planar/tetrahedron			
	Co	Ni	Co	Ni
M-N1 (Å)	2.066/2.050	2.014/2.036	2.091/2.027	2.054/2.009
M-N2 (Å)	2.085/2.050	2.027/2.036	2.092/2.049	2.054/2.045
M-N3 (Å)	2.063/2.050	2.027/2.036	2.093/2.044	2.054/2.020
M-N4 (Å)	2.087/2.050	2.014/2.036	2.093/2.034	2.054/2.031
C1-N1 (Å)	—	—	1.459/1.453	1.463/1.450
C2-N1 (Å)	1.327/1.328	1.326/1.326	1.339/1.339	1.337/1.337
C2-N2 (Å)	1.326/1.328	1.327/1.326	1.339/1.337	1.338/1.335
N1-M-N2 (degree)	64.59/65.54	66.18/65.75	64.34/65.48	65.40/65.66
N3-M-N4 (degree)	64.59/65.54	66.18/65.75	64.41/65.44	65.17/65.75
N1-N2-N3-N4 (degree)	0.89/84.62	0.00/84.57	0.015/85.11	0.019/83.28

minimize the possible effects of the steric hindrance arising from the side chains followed by structural minimization. The calculated bond parameters and total energies are shown in Tables I and II. The tetrahedron geometry is found to be overwhelmingly more stable than the planar configuration by as much as 56.48 kcal/mol and 31.38 kcal/mol for Co(H-HAMD)$_2$ and Ni(H-HAMD)$_2$, respectively, indicating that tetrahedron geometry is the dominant configuration for this ligand. Replacing ^{i}Pr groups with ^{t}Bu does not alter the relative stability (Table II). Our DFT calculations clearly indicate that the tetrahedron configuration is energetically preferred. Therefore, in the following, we present results only on structures with a tetrahedron configuration.

The complexation between the amidinate ligands and transition metal atoms is dictated by orbital interactions between ligands and metal atoms. The low-lying states of the ligands are comprised of π orbitals, whereas the frontier orbitals of metal atoms are dominated by 3*d* and 4*s* orbitals. In Figure 3, we use Co(^{i}Pr-MeAMD)$_2$ to schematically illustrate possible mixing of orbitals of low lying states between a metal atom and an amidinate ligand. The calculated HOMO and HOMO1 of the complex are also shown. The overlaps between the empty/partially empty 3*d* and 4*s* orbitals of Co and the ligand HOMO and between the occupied/partially occupied 3*d* orbitals of Co and the ligand LUMO, which leads to formation of two topmost occupied molecular orbitals of the complex, are readily visible. It is conceivable that functional group substitutions on the ligand would tune the orbital overlap strength, giving rise to various chelation strengths and complex stability.

TABLE II

The calculated total energy of planar and tetrahedron structures (unit: Hartree).

	Planar	Tetrahedron
Co(H-HAMD)$_2$	−444.785676	−444.879232
Co(^{i}Pr-MeAMD)$_2$	−995.096185	−995.108627
Co(^{t}Bu-MeAMD)$_2$	−1152.285404	−1152.332064
Ni(H-HAMD)$_2$	−469.910089	−469.962326
Ni(^{i}Pr-MeAMD)$_2$	−1020.220274	−1020.229876
Ni(^{t}Bu-MeAMD)$_2$	−1177.415281	−1177.440008

In general, for β-group migration, the amidinate complexes undergo a TS that leads to the formation of products except for M = Co, Ni; R = ^{i}Pr; R′ = Me (Fig. 2) for which the complexes undergo two lowest energy reaction pathways as shown in our previous communication [28]. The first is internal rotation of the side group (^{i}Pr) to orient an H atom toward the metal; subsequently, the H atom moves to the metal center to form a TS. The internal rotation requires approximately 1–2 kcal/mol only. The fully optimized TS structures of Co/Ni(^{i}Pr-MeAMD)$_2$ and Co/Ni(^{t}Bu-MeAMD)$_2$ are displayed in Figure 4. The main features of the calculated TS structures of other compounds are similar and thus not shown. The main optimized structure parameters are shown in Table III. The calculated H—Ni and CH_3—Ni bonds are

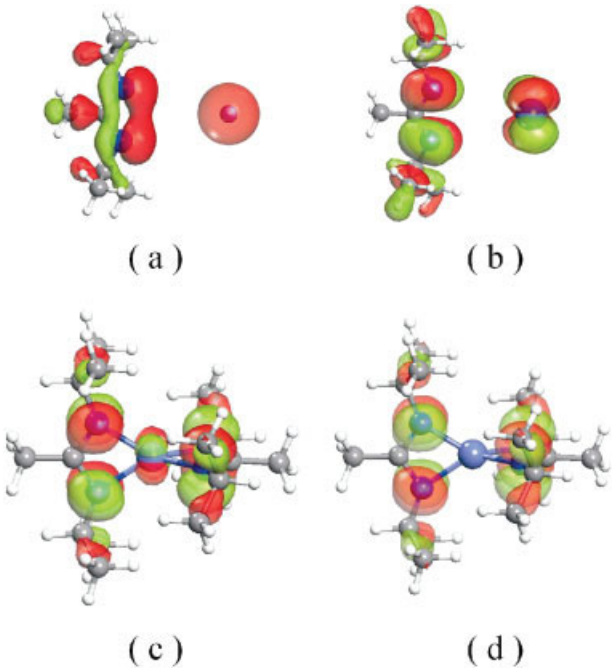

FIGURE 3. Orbital interactions in amidinate complexes. (a) σ bonding between amidiante ligand and metal atom, (b) δ bonding between amidinate ligand and metal atom, (c) HOMO of Co(^{i}Pr-MeAMD)$_2$, (d) HOMO1 of Co(^{i}Pr-MeAMD)$_2$. [Color figure can be viewed in the online issue, which is available at www.interscience.wiley.com.]

considerably shorter than the H—Co and CH_3—Co bonds, indicating stronger energetic preference of the β-migration groups toward Ni.

On β-migration, the complexes undergo substantial structural relaxation. The six-membered ring is broken and the side group, where β-migration occurs, which stretches away from the metal center. The bond order of C1—N1 changes from one to two and its affiliated ligand rotates considerably, allowing the product to adopt enough space to form a planar structure. The optimized structures of Co/Ni(^{i}Pr-MeAMD)$_2$ and Co/Ni(^{t}Bu-MeAMD)$_2$ are shown in Figure 5 and the main calculated bond parameters are listed in Table III. Again, the fully optimized structures of other products exhibit similar main features to those shown in Figure 5. Similar to the TS structures showing in Figure 4, the Ni—H and Ni—CH_3 bonds in Ni (^{i}Pr-MeAMD)$_2$ and Ni(^{t}Bu-MeAMD)$_2$ are much shorter than those in Co (^{i}Pr-MeAMD)$_2$ and Co(^{t}Bu-MeAMD)$_2$, suggesting that formation of Ni complexes would be easier.

The primary thrust of the present study is to understand factors that affect the reactivity of amidinate complexes toward β-migration. These include ligand chelation strength, ability to migrate, and metal affinity toward β-migration.

To quantitatively characterize the bond strength, we define in Eq. (1) the chelation energy as

$$E_{CE} = E_{Precursor} - 2 \times E_{ligand} - E_{metal} \qquad (1)$$

where $E_{precursor}$, E_{ligand}, and E_{metal} stand for energies of precursor, ligand, and metal atom, respectively. The calculated values of chelation energies of several selected amidinate complexes are shown in Table IV. It is clear that in general for a same ligand, chelation with Ni is considerably weaker than with Co. Electron rich groups attached to the N atoms give rise to stronger ligand-metal bonding. The effect of substitution at the C site of four-membered ring appears to be less important on the bonding.

To understand the effects of substitution groups on the ability of β-migration, we selected several amidinate compounds and calculated the reaction energies and activation barriers on β-migration as shown in Table V. Several important conclusions can be readily drawn from the following calculated data:

1. It is both thermodynamically and kinetically more favorable for β-migration to occur in Ni

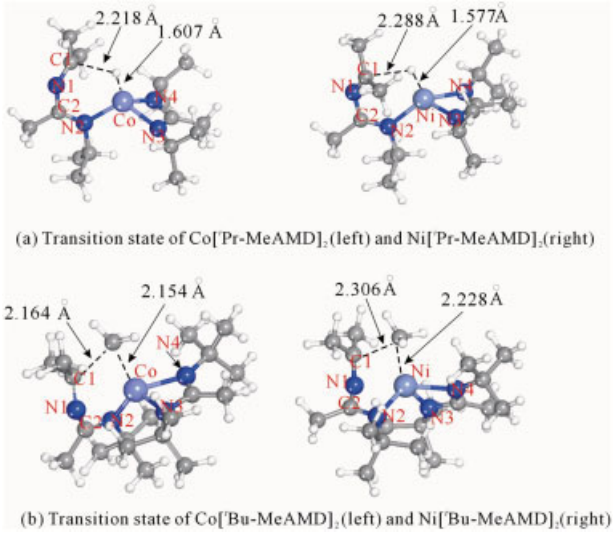

FIGURE 4. The optimized transition state structures of Co(^{i}Pr-MeAMD)$_2$ and Co(^{t}Bu-MeAMD)$_2$. [Color figure can be viewed in the online issue, which is available at www.interscience.wiley.com.]

TABLE III

Main bond parameters of the optimized structures of transition states and final products of Co(^{i}Pr-MeAMD)$_2$, Ni(^{i}Pr-MeAMD)$_2$, Co(^{t}Bu-MeAMD)$_2$, and Ni(^{t}Bu-MeAMD)$_2$.

	Co(^{i}Pr-MeAMD)$_2$		Ni(^{i}Pr-MeMAD)$_2$		Co(^{t}Bu-MeAMD)$_2$		Ni(^{t}Bu-MeAMD)$_2$	
	TS	Product	TS	Product	TS	Product	TS	Product
M-R (Å)	1.606	1.556	1.577	1.485	2.164	1.996	2.228	1.948
M-N1(Å)	3.179	3.192	3.241	3.085	2.603	2.882	2.192	2.660
M-N2 (Å)	2.041	1.927	2.041	1.901S	2.031	1.976	2.086	1.939
M-N3 (Å)	2.055	2.006	2.048	2.017	2.054	2.055	2.021	2.019
M-N4 (Å)	2.045	1.951	2.012	1.892	2.104	2.013	2.151	1.978
C1-N1 (Å)	1.300	1.286	1.294	1.285	1.363	1.285	1.344	1.290
C2-N1 (Å)	1.360	1.392	1.365	1.379	1.345	1.396	1.385	1.383
C2-N2 (Å)	1.316	1.300	1.310	1.306	1.325	1.297	1.301	1.302
R-M-N2 (degree)	108.26	88.79	104.92	89.31	110.39	88.36	107.92	88.99
N3-M-N4 (degree)	65.55	66.74	65.86	67.57	64.87	65.67	64.36	66.80
R-N2-N3-N4 (degree)	82.73	0.029	63.19	3.39	80.32	3.28	57.42	3.86

R represents β-H and β-CH_3, respectively.

complexes than in Co complexes regardless of migration groups. Although, in all cases, the migration process is endothermic, β-H migration in Ni(^{i}Pr-MeAMD)$_2$ is close to thermal neutral with a moderate activation energy, indicating the reaction could occur at a typical ALD condition. This is in good agreement with experimental observations [26].

2. Replacing the H atom with a CH_3 group substantially enhances the thermal stability with significantly higher activation barrier as seen in Bis(^{i}Pr-MeAMD)$_2$ (β-H) and Bis(^{t}Bu-MeAMD)$_2$ (β-CH_3) and in Bis(^{s}Bu-MeAMD)$_2$ (β-H) and Bis(^{s}Bu-MeAMD)$_2$ (β-CH_3). This is again consistent with experimental facts [26].
3. The stability of the complexes against β-migration increases with chelation strength as revealed in Tables IV and V.
4. For β-H migration with ^{i}Pr groups attached to the N atoms, increasing electron donating ability (from TFEt to Et) in general results in

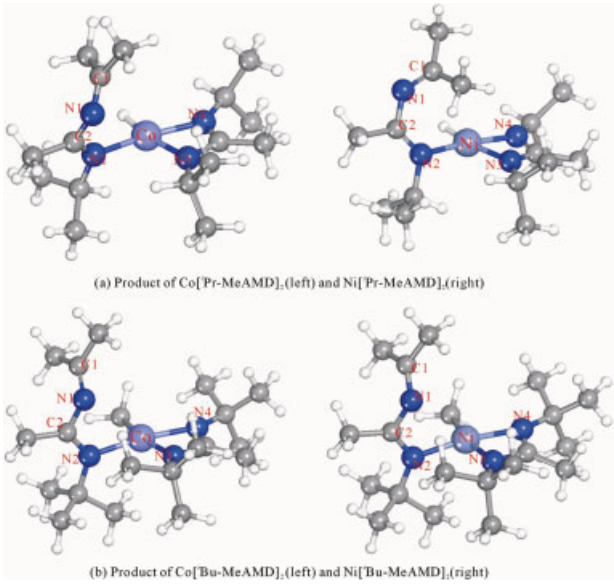

FIGURE 5. (a) Product structures of Co(^{i}Pr-MeAMD)$_2$ (left) and Ni(^{i}Pr-MeAMD)$_2$ (right), (b) product structures of Co(^{t}Bu-MeAMD)$_2$ (left) and Ni(^{t}Bu-MeAMD)$_2$. [Color figure can be viewed in the online issue, which is available at www.interscience.wiley.com.]

TABLE IV

The calculated chelation energy (E_{CE}) of amidinate ligand in Co (R-R′AMD)$_2$ (unit: kcal/mol).

	E_{CE}^{Co}	E_{CE}^{Ni}
(^{i}Pr-HAMD)$_2$	−184.9	−170.6
(^{i}Pr-MeAMD)$_2$	−189.0	−171.1
(^{i}Pr-EtAMD)$_2$	−206.7	−190.4
(^{i}Pr-TFEtAMD)$_2$	−192.0	−176.7
(^{t}Bu-MeAMD)$_2$	−200.9	−178.2
(^{t}Bu-EtAMD)$_2$	−208.4	−192.2

R represents isopropyl, butyl, respectively; R′ represents methyl and trifluoroethyl groups, respectively.

TABLE V

The calculated migration energies and barriers of several selected Co, Ni amidinate complexes.

	Cobalt		Nickel	
	ΔE_r	E_a	ΔE_r	E_a
Bis(^{i}Pr-MeAMD)$_2$ (β-H)	16.7	33.6	4.7	24.3
Bis(^{i}Pr-EtAMD)$_2$ (β-H)	16.5	31.6	9.1	33.8
Bis(^{i}Pr-TrifluoEtAMD)$_2$ (β-H)	13.2	28.6	7.9	28.1
Bis(^{s}Bu-MeAMD)$_2$ (β-H)	20.6	33.0	16.0	32.7
Bis(^{t}Bu-MeAMD)$_2$ (β-CH_3)	29.2	52.8	18.5	40.2
Bis(^{t}Bu-EtAMD)$_2$ (β- CH_3)	28.8	52.4	23.3	49.8
Bis(^{s}Bu-MeAMD)$_2$ (β-CH_3)	27.6	50.5	24.1	51.8

β-H and β-CH_3 represent the migrating groups (unit: kcal/mol).

higher thermal stability and reaction barrier, although the effect appears to be moderate.

5. Side group substitution, either at N or C, does not change the reaction energies and the activation energies significantly for Co complexes; however, it does influence the energetics for Ni complexes considerably, likely due to the fact that the weaker bonding between Ni atom and the migration species makes the Ni complexes more sensitive to the change of ligand environment.

The electronic structures of both Co and Ni amidinates with a tetrahedral configuration adopt high spin states with spin multiplicity of quartet for Co and triplet for Ni arising from the relatively weak ligand field. At the TSs, the spin states remain unchanged as shown in our previous communication [28]. On β-migration, substantial rearrangements of electronic structures take place as the metal atom adopts an electronic configuration from tetrahedron to square planar. For the Ni complexes, the unpaired electrons are quenched by the migrating species, forcing the molecules to adopt a spin-free ground electronic structure. Likewise, for the Co complexes, the number of unpaired electrons is reduced from 3 to 1. The low spin ground states of electronic structures are derived from the strong bonding between the metal atoms and the migrating groups. As a consequence of the change of spin states in the reaction process, potential energy curve crossing occurs. The details have been discussed previously [28]. The change of electronic structures of the amidinate compounds results in electron redistribution in these molecules. Table VI lists the calculated Hirshfeld charges of the metal atoms, the migration species and the chelating N atoms. In all cases, the β-migration leads to charge flow from the 4s orbital of the metal atoms to the migration species, forcing the metal atoms to withdraw charges from the electron lone pairs of the chelating N atoms. As a consequence, the positive charge on the metal atoms is significantly reduced. Indeed, Table VI indicates that the migrating species all gain charges from the metal atoms and the charges on the chelating N atoms decrease considerably on β-migration. In particular, Ni atom gains more charges than Co due to stronger Ni—H/Ni—CH_3 bonding, consistent with the more favorable reaction energies for Ni complexes.

Summary

Understanding of metal–ligand interactions and electronic structure of their compounds is of fundamental importance for design and development of novel precursors for semiconductor applications. In the present work, we have performed a series of quantum mechanical calculations using DFT to study structures and chemical reactivity resulting from β-migration for several selected amidinate-based Ni and Co complexes. Our results are consistent with the available experimental observations and provide useful insight into the thermal stability and kinetics of β-migration in these compounds.

TABLE VI

The calculated Hirshfeld charges in Co/Ni(^{i}Pr-MeAMD)$_2$ and Co/Ni(^{t}Bu-MeAMD)$_2$ before and after β-migration.

Precursors	Co(^{i}Pr-MeAMD)$_2$ before/after	Ni(^{i}Pr-MeAMD)$_2$ before/after	Co(^{t}Bu-MeAMD)$_2$ before/after	Ni(^{t}Bu-MeAMD)$_2$ before/after
M (M = Co, Ni)	0.260/0.086	0.244/−0.004	0.255/0.143	0.235/0.065
R (R = H, CH_3)	0.025/−0.156	0.024/−0.126	−0.018/−0.24	−0.016/−0.194
N	−0.150/−0.120	−0.150/−0.113	−0.151/−0.120	−0.150/−0.110

We first performed full optimizations on the ground states structures of the selected precursors. The calculated structural parameters are in excellent agreement with the available crystal structures. We subsequently proceeded to calculate structures of TSs and final products on β-migration. It was found that the bond distance between metal atoms and migrating groups is considerably shorter in Ni-based amidinate compounds than in Co-based compounds. As the migrating groups move close to the TSs, one of the M—N (M = Co, Ni) bonds gradually loses up and the metal atoms adopt a square planar configuration from a tetrahedron configuration, leading to the formation of a strong bond between metal atoms and the migrating groups.

Factors that influence the reactivity of amidinate compounds toward β-migration were carefully addressed. It was found that β-migration is more readily to take place in Ni complexes than in Co complexes regardless of migration groups. In particular, for Ni(^{i}Pr-MeAMD)$_2$, the β-H migration process is close to thermal neutral with a moderate activation energy and thus the reaction could occur at a typical ALD condition. This is in good agreement with experimental observations. Our calculations indicate that replacing the H atom with CH_3 as the migrating group can substantially enhance the thermal and kinetic stability, again consistent with the available experimental facts. Furthermore, stronger chelation strength enhances the complex stability against β-migration. We show that the reactivity of Co/Ni bis-amidnate complexes via β-group migration is significantly influenced by side group substitutions. Our results provide useful information for further development of novel precursors for semiconductor applications.

References

1. Li, B.; Sullivan, T. D.; Lee, T. C.; Badami, D. Microelectron Reliab 2004, 44, 365.
2. Holloway, K.; Fryer, P. M.; Cabral, C., Jr.; Harper, J. M. E.; Bailey, P. J.; Kelleher, K. H. J Appl Phys 1992, 71, 5433.
3. Manaud, J. P.; Poulon, A.; Gomez, S.; Le Petitcorps, Y. Surf Coat Technol 2007, 202, 222.
4. Elers, K.-E.; Saanila, V.; Soininen, P. J.; Li, W.-M.; Kostamo, J. T.; Haukka, S.; Juhanoja, J.; Besling, W. F. A. Chem Vap Deposition 2002, 8, 149.
5. Suh, B.-S.; Lee, Y.-J.; Hwang, J.-S.; Park, C.-O. Thin Solid Films 1999, 348, 299.
6. Wu, J.; Han, B.; Zhou, C.; Lei, X.; Gaffney, T. R.; Norman, J. A. T.; Li, Z.; Gordon, R.; Cheng, H. J Phys Chem C 2007, 111, 9403.
7. Kim, H.; Koseki, T.; Ohba, T.; Ohta, T.; Kojima, Y.; Sato, H.; Hosaka, S.; Shimogaki, Y. Appl Surf Sci 2006, 252, 3938.
8. Rohde, S. L.; Matthews, A. In Mechanical Engineers' Handbook (Third Edition); Myer, K., Ed.; Wiley: New York, 2006; p 396.
9. Chen, P.; Mitsui, T.; Farmer, D. B.; Golovchenko, J.; Gordon, R. G.; Branton, D. Nano Lett 2004, 4, 1333.
10. Rosenberg, R.; Edelstein, D. C.; Hu, C.-K.; Rodbell, K. P. Annu Rev Mater Sci 2000, 30, 229.
11. Ritala, M.; Leskelä, M. In Handbook of Thin Film Materials; Nalwa, H. S., Ed.; Academic Press: San Diego, 2002; p 103.
12. Farmer, D. B.; Gordon, R. G. Electrochem Solid-State Lett 2005, 8, G89.
13. Lim, B. S.; Rahtu, A.; de Rouffignac, P.; Gordon, R. G. Appl Phys Lett 2004, 84, 3957.
14. Gordon, R. G.; Barry, S. T.; Barton, J. T.; Broomhall-Dillard, R. N. R. Thin Solid Films 2001, 392, 231.
15. Hausmann, D. M.; Kim, E.; Becker, J.; Gordon, R. G. Chem Mater 2002, 14, 4350.
16. Biercuk, M. J.; Monsma, D. J.; Marcus, C. M.; Becker, J. S.; Gordon, R. G. Appl Phys Lett 2003, 83, 2405.
17. Gordon, R. G.; Hausamann, D.; Kim, E.; Shepard, J. Chem Vap Deposition 2003, 9, 73.
18. Li, Z.; Barry, S. T.; Gordon, R. G. Inorg Chem 2005, 44, 1728.
19. Hausmann, D. M.; de Rouffigna, P.; Smith, A.; Gordon, R.; Monsma, D. Thin Solid Films 2003, 443, 1.
20. Gordon, R. G.; Becker, J.; Hausmann, D.; Suh, S. Chem Mater 2001, 13, 2463.
21. Javey, A.; Guo, J.; Farmer, D. B.; Wang, Q.; Yenilmez, E.; Gordon, R. G.; Lundstrom, M.; Dai, H. Nano Lett 2004, 4, 1319.
22. Hausmann, D. M.; Gordon, R. G. J Crystal Growth 2003, 249, 251.
23. Musgrave, C. B.; Gordon, R. G. Future Fab Int 2005, 18, 126.
24. Päiväsaari, J.; Dezelah, C. L., IV; Black, B.; El-Kaderi, H. M.; Heeg, M. J.; Putkonen, M.; Niinistö, L.; Winter, C. H. J Mater Chem 2005, 15, 4224.
25. Duchateau, R.; van Wee, C. T.; Meetsma, A.; van Duijnen, P. T.; Teuben, J. H. Organometallics 1996, 15, 2279.
26. Lim, B. S.; Rahtu, A.; Park, J.-S.; Gordon, R. G. Inorg Chem 2003, 42, 7951.
27. Brussee, E. A. C.; Meetsma, A.; Hessen, B.; Teuben, J. H. Organometallics 1998, 17, 4090.
28. Wu, J.; Li, J.; Zhou, C.; Lei, X.; Gaffney, T.; Norman, J. A. T.; Li, Z.; Gordon, R. G.; Cheng, H. Organometallics 2007, 26, 2803.
29. Delley, B. J Chem Phys 2000, 113, 7756.
30. Delley, B. J Chem Phys 1990, 92, 508.
31. Perdew, J. P.; Wang, Y. Phys Rev B 1992, 45, 13244.
32. Halgren, T. A.; Lipscomb, W. N. Chem Phys Lett 1977, 49, 225.
33. Schmidt, J. A. R.; Arnold, J. J Chem Soc, Dalton Trans 2002, 3454.
34. Kawaguchi, H.; Matsuo, T. Chem Commun 2002, 958.
35. Hagadorn, J. R.; Arnold, J. Inorg Chem 1997, 36, 132.
36. Sadique, A. R.; Heeg, M. J.; Winter, C. H. J Am Chem Soc 2003, 125, 7774.
37. Nijhuis, C. A.; Jellema, E.; Sciarone, T. J. J.; Meetsma, A.; Budzelaar, P. H. M.; Hessen, B. Eur J Inorg Chem 2005, 2089.